mathematics

MDPI

Article

Electrostatic-Elastic MEMS with Fringing Field: A Problem of Global Existence

Paolo Di Barba [1], Luisa Fattorusso [2] and Mario Versaci [3,*]

[1] Dipartimento di Ingegneria Industriale e dell'Informazione, University of Pavia, Via A. Ferrata 5, I-27100 Pavia, Italy; paolo.dibarba@unipv.it
[2] Dipartimento di Ingegneria dell'Informazione Infrastrutture Energia Sostenibile, "Mediterranea" University, Via Graziella Feo di Vito, I-89122 Reggio Calabria, Italy; luisa.fattorusso@unirc.it
[3] Dipartimento di Ingegneria Civile Energia Ambiente e Materiali, "Mediterranea" University, Via Graziella Feo di Vito, I-89122 Reggio Calabria, Italy
* Correspondence: mario.versaci@unirc.it; Tel.: +39-09651692273

Abstract: In this paper, we prove the existence and uniqueness of solutions for a nonlocal, fourth-order integro-differential equation that models electrostatic MEMS with parallel metallic plates by exploiting a well-known implicit function theorem on the topological space framework. As the diameter of the domain is fairly small (similar to the length of the device wafer, which is comparable to the distance between the plates), the fringing field phenomenon can arise. Therefore, based on the Pelesko–Driscoll theory, a term for the fringing field has been considered. The nonlocal model obtained admits solutions, making these devices attractive for industrial applications whose intended uses require reduced external voltages.

Keywords: electrostatic MEMS; fringing field; nonlinear elliptic models; fourth-order integro-differential models; partial differential equations

Citation: Di Barba, P.; Fattorusso, L.; Versaci, M. Electrostatic-Elastic MEMS with Fringing Field: A Problem of Global Existence. *Mathematics* **2022**, *10*, 54. https://doi.org/10.3390/math10010054

Academic Editor: Alessandro Niccolai

Received: 29 November 2021
Accepted: 22 December 2021
Published: 24 December 2021

Publisher's Note: MDPI stays neutral with regard to jurisdictional claims in published maps and institutional affiliations.

Copyright: © 2021 by the authors. Licensee MDPI, Basel, Switzerland. This article is an open access article distributed under the terms and conditions of the Creative Commons Attribution (CC BY) license (https://creativecommons.org/licenses/by/4.0/).

1. Introduction

In recent years, scientific research has paid particular attention to the study of model descriptions with different levels of accuracy and detail, and to the behavior of micro-electro-mechanical systems (MEMSs) [1,2]. They are devices of various kinds (mechanical, electrical, and electronic) integrated in a highly miniaturized form onto the same substrate of semiconductor material (for example, silicon [3–5]) that combine the electrical properties of the semiconductor with the opto-mechanical properties. These are therefore "intelligent" systems that combine electrical [6], electronic [7], fluid management [8], optical [9], biological [10], chemical [11], and mechanical [12] functions in small spaces, associating all the possible management functions of a process to sensors and actuators [13].

Among them, electrostatic MEMSs with parallel metallic plates (one of which is fixed and the other deformable when an external electrical voltage V is applied) stand out, as they are versatile and easy to manufacture [1,2]. Many models have been formulated for electrostatic MEMSs with parallel metallic plates considering all the physical-technical specifications [1,2,13,14]. The physical-mathematical modeling of MEMS is particularly useful since, on the one hand, it allows for the evaluation of the mechanical tension states of the elements responsible for the deformation as a function of the intended use of the device (and vice versa) [6], and on the other hand, it permits the carrying out of predictive functionality tests which, when carried out on the real device, could lead to the destruction of the device itself [15]. Furthermore, unlike the works known in the literature concerning the physical-mathematical modeling of MEMS with parallel plates (according to our knowledge) [1], it is necessary to take into account the phenomenon of the fringing field, which is quite frequent in some industrial MEMS devices and whose main problem is the excessive deformation of the deformable element, with the consequent risk of touching the upper plate that would then cause unwanted electrostatic discharges; should these

discharges be of strong intensity, this could lead to the destruction of the device [16]. In the recent past, authors have been interested in physical-mathematical models for MEMS membrane devices for industrial applications (where the amplitude of the electric field has been shown to be locally proportional to the curvature of the membrane) in which the effects of the fringing field were taken into account (see [6] and references within it). The fringing field phenomenon, which is mainly dependent on the fact that the order of amplitude of the length of the device is comparable to the order of magnitude of its width, involves the bending of the lines of force of the electric field between the two plates near the boundaries while they remain parallel as one moves inward [1,16]. Among them, the fourth-order integro-differential model studied extensively in [14] stands out; it has led to the achievement of interesting results with a global existence. However, the model studied in [14], although mathematically interesting, is not very attractive for engineering applications due to the mathematical formulation that characterizes it, which does not reconcile with the physical behavior of some components of the device (see [1,2,13]). Therefore, in this paper, starting with an adaptation of the model studied in [14] (so that it is more adherent to the physics of industrially produced devices), we present a new general N-dimensional model in which, by exploiting the Pelesko–Driscoll theory [17], the additive term $\lambda\delta|\nabla u(x)|^2$ represents the effect due to the fringing field. The model is the following:

$$\begin{cases} \Delta^2 u(x) = \left(\beta \int_\Omega |\nabla u(x)|^2 \mathrm{dx} + \gamma\right)\Delta u(x) + \\ + \dfrac{\lambda f(x)}{(1-u(x))^2\left(1+\chi\int_\Omega \frac{\mathrm{dx}}{(1-u(x))}\right)^2} + \lambda\delta|\nabla u(x)|^2 \\ u(x) = 0, \quad \nabla u(x) = 0 \quad x \in \partial\Omega, \\ 0 < u(x) < 1 \quad x \in \Omega \subset \mathbb{R}^N, \quad N < 4. \end{cases} \tag{1}$$

In (1), Ω is a smooth bounded domain, while the profile of the deflecting plate, $u : \Omega \to \mathbb{R}$, is a smooth unknown function. Moreover, the dielectric properties of the material constituting the plates of the MEMS are taken into account by a bounded function, $f : \Omega \to \mathbb{R}^+$. Furthermore, λ is a positive parameter which represents the drop voltage between the deflecting plate and the upper plate, and β, γ, and χ are a set of positive parameters related to the stiffness of the deflecting plate, to the material deformation producing self-stretching phenomena, to the tangential tension forces, and the nonlocal dependence of the electrostatic potential on the solution due to any non-uniform electric charge distribution. Finally, δ is a positive constant that weighs the effect due to the fringing field phenomenon.

In the past, many models considering the fringing field [6,17,18] have been proposed and studied. However, they studied simplified versions of more complex analytical models that did not fit in well with the demands of the industrial world.

Therefore, here, we propose the study of the global existence of (1), offering novel insights of engineering interest.

The remainder of the paper is organized as follows. The following Section offers a brief overview of the genesis of the mathematical model of the parallel plate MEMS device, with particular reference to devices affected by the fringing field. Section 3 highlights some advantages and disadvantages of the proposed model. Afterward (Section 4), the main result presented in this paper, which concerns the global existence and uniqueness of (1), is stated. Once the Existence and Uniqueness Theorem for the solution has been stated, some physical-engineering considerations are highlighted in Section 5. Subsequently, a well-known theorem on topological spaces is recalled while the proof of our main result is detailed in Section 6. Finally, some conclusions and future perspectives are drawn.

2. Genesis of the Model with the Fringing Field

In its 3D representation, the MEMS device studied here represents an electrostatic-elastic system consisting of two parallel plates of the same material with equal and finite thickness. One of the plates, the fixed ground plate, is at reference electrical potential

($V = 0$), while the elastic plate, with supported boundary, deforms toward the fixed ground plate without touching it (to avoid unwanted electrostatic discharges). Figure 1 depicts a $3D$ schematic of the MEMS device in which the lower plate (deformable) is represented in its resting position.

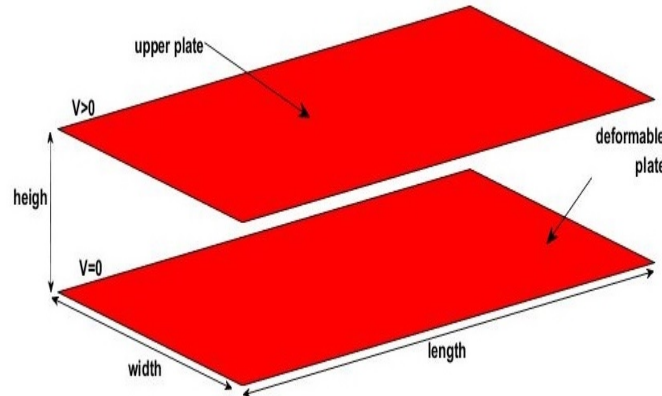

Figure 1. $3D$ schematic of the MEMS device with parallel plates.

Therefore, the electrostatic potential, ϕ, as is known from classical electrostatics [1], satisfies $\Delta\phi = 0$ (Laplace's equation) everywhere between the plates and in the region surrounding the device [1,19]. Modeling the deformable platelby exploiting the plate theory in steady-state conditions (well-known in the literature [1,19]) and by indicating the load function with $\tilde{F}(x)$, $u(x)$ satisfies the following equations:

$$\tilde{K}_1(x)\Delta^2 u(x) = \tilde{K}_2(x)\Delta u(x) + \tilde{F}(x), \tag{2}$$

where $\tilde{K}_1(x)$ and $\tilde{K}_2(x)$ are specific weight functions defined below.

Remark 1. *From a strictly engineering point of view, $\tilde{F}(x)$ has a very important meaning because locally, it establishes how the deformable plate is stressed when the external V is applied. In the case under study, V determines an electrostatic field inside the device that locally generates an electrostatic force, and consequently, electrostatic pressure that acts on the plate and deforms it towards the upper one. This deformation, however, must be such as to avoid any contact between the two plates (in order to avoid any unwanted electrostatic discharges). It follows that $\tilde{F}(x)$ must be closely related both to V (so that the deformation of the deformable plate can be controlled by V) and to the dielectric, mechanical, and geometric properties of the deformable plate.*

According to Remark 1, if d is the distance between the plates and L represents the length of the device, and if T represents the mechanical tension of the deformable plate at rest and ϵ_0 is the permittivity of the free space, by exploiting the scaling operation to achieve a dimensionless model, $\tilde{F}(x)$ assumes the following form [1]:

$$\tilde{F}(x) = \frac{\lambda f(x)}{(1 - u(x))^2}, \tag{3}$$

with

$$\lambda = \frac{\epsilon_0 V^2 L^2}{2d^3 T} \tag{4}$$

which represents the tuning parameter of the device (because it is directly linked to V, T, L, and d). Thus, (2) becomes:

$$\tilde{K}_1(x)\Delta^2 u(x) = \tilde{K}_2(x)\Delta u(x) + \frac{\lambda f(x)}{(1 - u(x))^2}. \tag{5}$$

Remark 2. *Equation (3), by exploiting (5), is not able to electrically control the device because industrially, V must be controlled to avoid the sudden elevation of the deformable plate [1]. For example, a basic capacitive control device can be exploited to solve this problem.*

According to Remark 2, a basic capacitive control device is constituted by a circuit whose elements are the series of source voltage, V_s, the capacitance of the fixed series capacitor, C_f, and finally, the MEMS device can be exploited (see Figure 2).

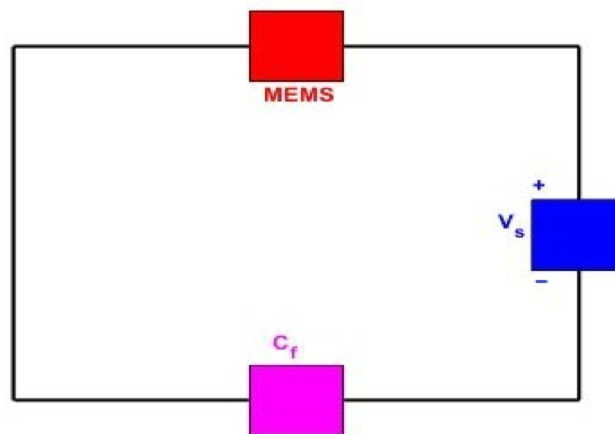

Figure 2. The basic capacitive control circuit.

Therefore, exploiting the theory of electrical circuits, the voltage drop, V, across the device becomes the following equation:

$$V = \frac{V_s}{1 + \frac{C}{C_f}} \tag{6}$$

where C is the capacitance of the MEMS device that is computable as follows:

$$C = \frac{\epsilon_0}{V} \int_\Omega \nabla\phi \cdot \hat{n} \mathrm{d}x \approx \frac{\epsilon_0}{V} \int_\Omega \frac{\partial \phi}{\partial z} \mathrm{d}x \approx \frac{\epsilon_0 L^2}{d} \int_\Omega \frac{\mathrm{d}x}{(1 - u(x))}. \tag{7}$$

Therefore, (6) becomes the following:

$$V = \frac{V_s}{1 + \frac{\epsilon_0 L^2}{C_f d} \int_\Omega \frac{\mathrm{d}x}{(1-u(x))}} \tag{8}$$

and setting

$$\chi = \frac{\epsilon_0 L^2}{C_f d} \tag{9}$$

Equation (6) is writable as follows:

$$V = \frac{V_s}{1 + \chi \int_\Omega \frac{dx}{(1-u(x))}} \tag{10}$$

from which

$$\left(\frac{V}{V_s}\right)^2 = \frac{1}{\left(1 + \chi \int_\Omega \frac{\mathrm{d}x}{(1-u(x))}\right)^2}. \tag{11}$$

Electrostatically, $\left(\frac{V}{V_s}\right)^2$ in (11) is the control action on the load; therefore, (3) becomes:

$$\tilde{F}(x) = \frac{\lambda f(x)}{(1-u(x))^2}\left(\frac{V}{V_s}\right)^2 = \frac{\lambda f(x)}{(1-u(x))^2\left(1+\chi\int_\Omega \frac{\mathrm{dx}}{(1-u(x))}\right)^2}. \tag{12}$$

Finally, putting (12) into (2), one achieves the following equation:

$$\tilde{K}_1(x)\Delta^2 u(x) = \tilde{K}_2(x)\Delta u(x) + \frac{\lambda f(x)}{(1-u(x))^2\left(1+\chi\int_\Omega \frac{\mathrm{dx}}{(1-u(x))}\right)^2}. \tag{13}$$

Remark 3. *χ, by definition, essentially depends on the calculation of the capacitance. Furthermore, as proved in [1], $\chi \in [0,1)$ because when $\chi \to 1^-$, the obvious bifurcation phenomena take place, which, as is known, could cause phenomena of structural instability that bring about, in extreme cases, the breakage of the device.*

Remark 4. *It is known that $\frac{\partial u}{\partial x}$ and $\frac{\partial u}{\partial y}$ represent the flexional curvatures, while $\frac{\partial u}{\partial z}$ represents the torsional curvature [1]. Hence, Δu, locally, consider all the curvatures. Moreover, since the horizontal position of the plate is fixed on $\partial\Omega$, a stretching phenomenon occurs. In this way, the slab is anchored on the edges so that its deformation under the action of the external V necessarily implies an increase in its surface. Therefore, in the hypothesis of elastic regimes of the deformation plate, the elastic return force will be proportional to the surface increase, with consequent stretching energy computable as follows [1]:*

$$\tilde{K}_2(x) = E_S(u(x)) = \beta\int_\Omega |\nabla u(x)|^2 dx. \tag{14}$$

Moreover, if γ is the stretching parameter, we also need to consider the tangential tension forces so that:

$$E_S(u(x)) = \beta\int_\Omega |\nabla u(x)|^2 dx + \gamma = \tilde{K}_2(x). \tag{15}$$

Finally, (13) can be written as follows:

$$\begin{aligned}\tilde{K}_1(x)\Delta^2 u(x) = &\left(\beta\int_\Omega |\nabla u(x)|^2 dx + \gamma\right)\Delta u(x) + \\ &+ \frac{\lambda f(x)}{(1-u(x))^2\left(1+\chi\int_\Omega \frac{dx}{(1-u(x))}\right)^2}.\end{aligned} \tag{16}$$

Remark 5. *Usually, $\tilde{K}_1(x)$ assumes the following expression [1,19]:*

$$\tilde{K}_1(x) = \frac{D}{L^2 T} \tag{17}$$

where D is the flexural rigidity of the material constituting the deformable plate. Experimentally, for the most used materials in the industry, $\tilde{K}_1(x) \approx 1$.

Finally, the model becomes:

$$\begin{cases}\Delta^2 u(x) = \left(\beta\int_\Omega |\nabla u(x)|^2 dx + \gamma\right)\Delta u(x) + \frac{\lambda f(x)}{(1-u(x))^2\left(1+\chi\int_\Omega \frac{\mathrm{dx}}{(1-u(x))}\right)^2} \\ u(x) = 0, \quad \nabla u(x) = 0 \quad x \in \partial\Omega, \\ 0 < u(x) < 1 \quad x \in \Omega \subset \mathbb{R}^3.\end{cases} \tag{18}$$

In the past, (18) has been studied extensively, as evidenced by the numerous scientific works published recently. In particular, global existence studies have been made for nonlocal MEMSs modeled by (18), with particular reference to bifurcation problems (see [1,19] and references therein).

Remark 6. *The authors of [20] have proved that* (18) *admits the following N-dimensional generalization:*

$$\begin{cases} \Delta^2 u(x) = \left(\beta \int_\Omega |\nabla u(x)|^2 dx + \gamma\right)\Delta u(x) + \dfrac{\lambda f(x)}{(1-u(x))^2\left(1+\chi\int_\Omega \frac{dx}{(1-u(x))}\right)^2} \\ u(x) = 0, \quad \frac{\partial u(x)}{\partial \eta} = 0, \quad x \in \partial\Omega, \\ 0 < u(x) < 1 \quad x \in \Omega \subset \mathbb{R}^N \end{cases} \tag{19}$$

According to our knowledge, (19) *has not yet been studied, except in particular cases, which has led to a considerable simplification of its formulation [1,19,20]. However, in [14], global existence was investigated for nonlocal MEMSs whose generalized model was the following equation:*

$$\begin{cases} \Delta^2 u(x) = \left(\beta \int_\Omega |\nabla u(x)|^2 dx + \gamma\right)\Delta u(x) + \dfrac{\lambda f(x)}{(1-u(x))^\sigma\left(1+\chi\int_\Omega \frac{dx}{(1-u(x))^\sigma}\right)} \\ u(x) = \Delta u(x) - du_\nu = 0, \quad x \in \partial\Omega, \quad d \geq 0 \\ 0 < u(x) < 1 \quad x \in \Omega \subset \mathbb{R}^N \\ \sigma \geq 2 \end{cases} \tag{20}$$

If one is interested in non-Coulomb potentials, in (20)*,* $\sigma > 2$*; otherwise,* $\sigma = 2$ *if the Coulombian potential is considered. However, although* $\sigma > 2$ *is mathematically interesting, for electrostatic MEMS, it assumes little interest (non-Coulomb potentials are very interesting when cosmic distances are considered); thus,* $\sigma = 2$ *would be the obvious choice. Finally, it is worth nothing that* (20)*, although mathematically interesting, finds little practical application in industrial realities [1,19].*

In both (19) and (20), no terms are present due to the fringing field. As is known, most MEMS devices are characterized by an L/d ratio such that inside and near the boundaries, the lines of force of the electric field bend. This electrostatic phenomenon, known as the fringing field, is considerably attenuated in the central area of the device until it is extinguished in the middle (for reasons of symmetry) [6,17]. According to the Pelesko–Driscoll theory [17], the term that takes into account the effects of the fringing field is writable as follows:

$$\lambda F\left(u(x), \frac{\mathrm{d}u(x)}{\mathrm{d}x}, \delta, \ldots\right) \tag{21}$$

where $F\left(u(x), \frac{\mathrm{d}u(x)}{\mathrm{d}x}, \delta, \ldots\right)$ is a suitable bounded function that describes the effects due to the fringing field close to the edges (canceling in the middle), and $\delta \geq 0$ is the factor that weighs the effect due to the fringing field. Pelesko and Driscoll proved that (21) becomes the following equation:

$$\lambda\delta|\nabla u(x)|^2 \tag{22}$$

which turned out to be additive, with the addend contained as a factor $\Delta u(x)$.

Therefore, according to Remark 6 and the Pelesko–Driscoll theory, (1) becomes the physical-mathematical model for MEMSs with parallel plates that is closest to industrial reality. Basically, the fringing field is an electrostatic phenomenon, according to which, due to the effect of V, the bending of $\mathbf{E}$ occurs at the edges of the MEMS, while at its center, $\mathbf{E}$ remains parallel. Under these conditions, the electrostatic capacity of the device undergoes substantial variations and can be formulated using empirical formulations [1,19]. In the recent past, many interesting results have been obtained regarding mathematical models of MEMSs with fringing fields. However, they essentially concern studies carried out on

simplified models ([18] and references therein) or those related to membrane devices ([6] and references therein).

Remark 7. *It is worth noting that this model, even if it represents a detailed physico-mathematical description of the device under study, does not take into account all the physical phenomena that take place in it (i.e., any additional non-linearities due to stress-excessive local mechanics, bifurcations, . . .). Thus, studying (1) automatically introduces an uncertainty that we, at the present stage, are not able to quantify but will surely be the subject of intense study in the future.*

3. Advantages and Disadvantages of the Model Under Study

The physico-mathematical model presented here, as is evident, has the undoubted advantage of taking into account many physical phenomena that occur inside an electrostatic MEMS with parallel plates when an external electrical voltage V is applied. Particularly, these advantages are listed below:

1. The model takes into account the effects due to the fringing field by means of an additive term that depends on $|\nabla u(x)|$. This dependence is, from an engineering point of view, very interesting since it allows for a consideration of the effects caused by the fringing field by means of a term that can be easily implemented both via software (for any numerical modeling) and via hardware. Furthermore, the presence of λ allows these effects to be controllable in voltage.
2. Concerning the model under study, it is worth underlining the fact that scientific results regarding the stability of its solutions are lacking. This could be dangerous if the unstable solutions were profiles $u(x)$ such that $\max\{u(x)\}$ would be close to the upper plate, triggering probable electrostatic discharges. However, since the device is controlled in voltage by (4) (and the model takes this into account through the presence of λ in the individual addends), it will be the intended use of the device to ensure that the electrostatic discharge effects are avoided. It follows that the most suitable industrial applications for MEMS devices governed by the physical-mathematical model under study are those for which the external voltages are reduced (i.e., biomedical applications).
3. In industrial applications, MEMS devices can be subject to fatigue phenomena due to the continuous use of the device, which subjects the deformable plate to continuous raising and lowering, with the evident hyper-stress of this deformable element (such as stiffness and self-stretching). Due to the presence of β and γ, the model presented takes into account the effects caused by these phenomena, making this physico-mathematical formulation more consistent with the physics of the devices.
4. In industrial MEMS devices with parallel plates, once the plate deforms, the electrostatic capacitance inside the device changes. It follows that this variation, from the theory of electrostatics, must be dependent on the geometric parameters of the device and on an additional electrostatic capacitance (i.e., C_f) that opposes the abrupt variations of V. The model presented in this paper takes this important phenomenon into account by means of the term weighted by χ.
5. The dielectric properties of the plates are also well-represented in the model by $f(x)$, which, for obvious physical reasons, is supposed to be bounded. Furthermore, $f(x)$ appears in the "capacitive" addend of the model where the dielectric properties of the material constituting the plates of the device are actually involved.

However, the model has some obvious disadvantages, which can be summarized as follows:

1. While λ is directly controllable by V (see (4) and the electrical circuit depicted in Figure 2), concerning $\delta \in \mathbb{R}^+$, nothing can be said about its possible limitations (as obtained in the past for electrostatic MEMS membranes [6]). In other words, at present, we are not able to control δ in order to weigh the effects caused by the fringing field in a controlled way.

2. Obviously, the model presented in this paper is static and has no dynamic component. Therefore, at present, we are not able to evaluate $u(x,t)$, with t being a time variable, especially in transitory conditions (such as the start of the deformable plate).
3. The model presented in this paper does not allow for the explicit acquisition of $u(x)$. Therefore, we must be satisfied with the obtaining conditions that ensure the existence and uniqueness of the solution. Obviously, suitable numerical techniques could be used, which, when applied to the model under study, provide an approximate solution. However, it is worth noting that these approximate solutions could represent the dreaded ghost solutions if they did not respect the conditions of existence and uniqueness mentioned above. Therefore, it seems logical to perform an analytical study of the model beforehand in order to obtain these conditions, leaving the acquisition of the approximate solutions to future work.

4. Statement of the Global Existence Theorem

The results obtained in [20] concern the solution to the semilinear biharmonic equation achieved when $\beta = \gamma = \chi = 0$ in (1) with Dirichlet boundary conditions when Ω is a ball of $\mathbb{R}^N$, $N < 8$. Moreover, we set the following:

$$\begin{cases} G(\beta,\gamma,u(x)) = \left(\beta \int_\Omega |\nabla u(x)|^2 \mathrm{dx} + \gamma\right)\Delta u(x) \\ g(\chi,u(x)) = \left(1 + \chi \int_\Omega \frac{\mathrm{dx}}{(1-u(x))}\right)^2 \\ F(\beta,\gamma,\chi,f,y(x),\delta) = \\ = \Delta^2 y(x) - G(\beta,\gamma,y(x)) - \frac{\lambda f(x)}{(1-y(x))^2 g(\chi,y(x))} - \lambda\delta|\nabla y(x)|^2. \end{cases} \tag{23}$$

Now, we present the our main result.

Theorem 1. *Let us consider a smooth bounded domain $\Omega \subset \mathbb{R}^N$, with $N < 4$ on which to consider the problem (1). Moreover, let us consider $f(x) \in L^\infty(\Omega)$ and α, β, γ, $\chi > 0$. Then, there exists $\lambda^* \ni' \forall\lambda \in (0,\lambda^*)$, problem (1) has a solution $u \in H^4(\Omega)$ with the diameter of Ω, d_Ω , and sufficiently small ($d_\Omega \ll 1$) and $\delta \in (0,+\infty)$.*

5. Some Physical Considerations on the Statement of Theorem 1

Theorem 1, besides having an undoubtedly mathematical meaning, has a strong impact in practice. To verify this, let us analyze all assumptions.

1. Ω, which represents the deformable plate of most industrially produced devices and has dimensions of the order of 10^{-6}, takes place. Therefore, the diameter of the domain can be considered as $\ll 1$.
2. Theorem 1 sets the restriction $N < 4$, which is a stronger restriction than $N < 8$ presented in [21]; it is natural to ask why this restriction is stronger than the one for which the results proved in [21] have been obtained. In the proof of Theorem 1 (see Section 6), the reason for this restriction will be clarified. However, we highlight that this restriction really does not affect the validity of the work for the industry that requires $3D$ representations.
3. The assumption $f(x) \in L^\infty(\Omega)$ requires that $f(x)$ is a measurable function such that

$$||f||_\infty = \inf\{S \geq 0 \ : \ |f(x)| \leq S \ \ a.e.\}. \tag{24}$$

   Then, $\forall x \in \Omega$ (i.e., for each point of the deformable plate), $|f(x)| \leq S$. Since $f(x)$ is the function holding the electromechanical properties of the material constituting the plates, it is necessary that these properties can be measured. Furthermore, such properties are positive and finite quantities for which (24) makes sense.
4. Theorem 1 states that $\exists\lambda* \ni' \forall\lambda \in (0,\lambda*)$, and problem (1) has a solution $u \in H^4(\Omega)$. The reason why λ must be less than $\lambda*$ lies in the fact that λ, in industrial reality,

represents the pull-in voltage, i.e., the value of λ such that no solution exists for any $\lambda \geq \lambda*$.

5. Finally, Theorem 1 requires that $u \in H^4(\Omega)$. In other words, u together with its derivatives up to the fourth order must be continuous. Then, from the geometric point of view, the higher order curvatures must remain continuous. This condition physically translates into the fact that the lower plate, during the movement towards the upper plate, must not undergo sudden deformations which would locally lead to the creation of defects such as making the device useless.

Remark 8. *We observe that Theorem 1 provides solutions for a fixed* $0 < \lambda < \lambda^*$ *such that:*

$$||u_\lambda||_\infty \leq C < 1. \tag{25}$$

Consequently, the smoothness of u_λ *follows the theory of elliptic regularity.*

To prove Theorem 1, we exploit the main result on tolopological spaces proved in [22].

6. Proof of Theorem 1

We propose to prove the existence and uniqueness of the solution of problem (1) by applying the result in [22]. For this purpose, we need to introduce the following definitions. As in [14], let us consider the following set:

$$X = \mathbb{R}^+ \times \mathbb{R}^+ \times \mathbb{R}^+ \times \{f \in L^\infty(\Omega) \ : \ |x \ : \ f(x) > 0| \neq 0\} \tag{26}$$

Let us also consider the following set:

$$Y = \left\{ u \in H^4(\Omega) \cap H_0^1(\Omega) \ : \quad 0 < u < 1, \ \int_\Omega \frac{\mathrm{dx}}{(1-u)^{16}} < M, \right. \tag{27}$$
$$\left. \int_\Omega |\nabla u|^4 \mathrm{dx} < M_2 \ \text{ and } \int_\Omega |\Delta u|^2 \mathrm{dx} < M_1, \ \ M, M_1, M_2 > 0 \right\}.$$

where M, M_1, and M_2 are suitable positive constants. Furthermore, we set the following:

$$Z = L^2(\Omega), \quad B = \Delta^2, \tag{28}$$

Moreover, we denote by x_0 the element belonging to X:

$$x_0 = (0, 0, 0, f_0) \tag{29}$$

and by $y_0 \in Y$, the element is such that:

$$u_0 = y_0(0, 0, 0, f_0) = y_0(x_0) \tag{30}$$

where u_0 is the solution of the following equation:

$$\begin{cases} \Delta u_0 = \frac{\lambda f_0}{(1-u_0)^2} + \lambda\delta|\nabla u_0|^2 & \text{on } \Omega \\ 0 < u_0 < 1 \\ u_0 = 0 & \text{on } \partial\Omega. \end{cases} \tag{31}$$

that exists, as proved in [18]. We observe in [18] that the proof has been obtained with $f_0 = 1$. Without losing the validity of the result, in this paper, we consider $f_0 \in L^\infty(\Omega)$; indeed, we can easily verify that the proof is identical.

Now, we prove here that the assumptions of the result in [22] are verified:

- Assumption (i): Referring to Theorem 1 in [18], we know that a solution for (31) exists, and it is unique if $\forall \lambda \leq \lambda^* = \lambda^*(f_0, \delta)$. Therefore, in our case, we can write the following equation:

$$F(x_0, u_0) = 0. \tag{32}$$

- Assumption (iv): This is also satisfied because B, as defined in (28), is injective on Y.
- Assumption (ii): We will verify that:

$$x \to F(x, y_0) \tag{33}$$

is continuous at x_0. In fact, considering that f carries the dielectric properties of the material constituting the plates of the device, and δ (terms that weights the fringing field phenomenon) is a positive constant that does not change, we can write the equation as follows:

$$\begin{aligned}
&\int_\Omega |F(x, y_0) - F(x_0, y_0)|^2 \mathrm{dx} = \\
&= \int_\Omega \bigg| \Big(\beta \int_\Omega |\nabla y_0|^2 dx + \gamma\Big) \Delta y_0 - \\
&- \frac{\lambda f}{(1-y_0)^2 g(\chi, y_0)} + \frac{\lambda f_0}{(1-y_0)^2} + \\
&+ \lambda \delta |\nabla y_0|^2 + \frac{\lambda f_0}{(1-y_0)^2 g(\chi, y_0)} - \\
&- \lambda \delta |\nabla y_0|^2 - \frac{\lambda f_0}{(1-y_0)^2 g(\chi, y_0)} \bigg|^2 \mathrm{dx} \leq \\
&\leq 2 \int_\Omega \left| \left(\beta \int_\Omega |\nabla y_0|^2 \mathrm{dx} + \gamma\right) \Delta y_0 \right|^2 + \\
&+ \left| \frac{\lambda (f - f_0)}{(1-y_0)^2 g(\chi, y_0)} \right|^2 \mathrm{dx} + \left| \frac{\lambda f_0}{(1-y_0)^2 g(\chi, y_0)} \right|^2 \leq \\
&\leq 4\beta^2 \Big(\int_\Omega |\nabla y_0|^2 \mathrm{dx} \Big)^2 \int_\Omega |\Delta y_0|^2 \mathrm{dx} + 4\gamma^2 \int_\Omega |\Delta y_0|^2 \mathrm{dx} + \\
&+ 4\lambda^2 ||f - f_0||^2_{\infty,\Omega} \int_\Omega \frac{1}{(1-y_0)^2} \mathrm{dx} + \\
&+ 4|\Omega| \chi^2 ||f_0||^2_{\infty,\Omega} \lambda^2 \int_\Omega \frac{1}{(1-y_0)} \mathrm{dx}.
\end{aligned} \tag{34}$$

Through this, (ii) is verified because as $x \to x_0$, $f \to f_0$, $\beta = \gamma = \chi = 0$ (see (29)).
- Assumption (v): Taking into account that Δ^2 is an isomorphism between $H^4(\Omega) \cap H^1_0(\Omega)$ and $L^2(\Omega)$, and because $Y \neq \emptyset$ is an open subset of $H^4(\Omega) \cap H^1_0(\Omega)$, by exploiting Remark 8, we can verify that if $I \subset Y$ is a neighborhood (open set) of y_0 whose radius is σ, $B(I)$ is also a neighborhood (open set) of $z_0 = B(y_0)$ whose radius is σ.

Indeed, by applying Sobolev's immersion theorem because $N < 4$, we can write the equation as follows:

$$H^4(\Omega) \hookrightarrow C^0(\overline{\Omega}). \tag{35}$$

Let us now consider $z = B(y)$, where y is an element of Y, with $||y - y_0||_{H^4(\Omega)} < \sigma$; then if we consider $z \in B(Y)$, we have:

$$||z - z_0||_{L^2(\Omega)} = ||B(y) - B(y_0)||_{L^2(\Omega)} \leq ||y - y_0||_{H^4(\Omega)} < \sigma. \tag{36}$$

In other words, $B(Y)$ is a neighborhood of z_0.

- Finally, we verify Assumption (iii). Without losing generality, we provide the proof for $k_1 = 1$; let us consider all the $y_1, y_2 \in Y$ solutions of the problem,. Thus, we can write the following equation:

$$\begin{aligned}
&\int_\Omega \Big| B(y_1) - B(y_2) - (F((\beta,\gamma,\chi,f,y_1) - F(\beta,\gamma,\chi,f,y_2)) \Big|^2 \mathrm{dx} = \\
&= \int_\Omega \Bigg| \Delta^2 y_1 - \Delta^2 y_2 - \Delta^2 y_1 + G(\beta,\gamma,y_1) + \frac{\lambda f}{(1-y_1)^2 g(\chi,y_1)} + \\
&+ \lambda\delta|\nabla y_1|^2 + \Delta^2 y_2 - G(\beta,\gamma,y_2) - \frac{\lambda f}{(1-y_2)^2 g(\chi,y_2)} - \lambda\delta|\nabla y_2|^2 \Bigg|^2 \mathrm{dx} \leq \\
&\leq \underbrace{2\int_\Omega \Big| G(\beta,\gamma,y_1) - G(\beta,\gamma,y_2) \Big|^2 \mathrm{dx}}_{I_1} + \\
&\underbrace{+\, 2\lambda^2 \int_\Omega |f|^2 \left| \frac{1}{(1-y_1)^2 g(\chi,y_1)} - \frac{1}{(1-y_2)^2 g(\chi,y_2)} \right|^2 \mathrm{dx}}_{I_2} \\
&+ \underbrace{2\lambda^2\delta^2 \int_\Omega \Big| |\nabla y_1|^2 - |\nabla y_2|^2 \Big|^2 \mathrm{dx}}_{I_3}.
\end{aligned} \tag{37}$$

Now, we compute I_1.

$$\begin{aligned}
I_1 &= \int_\Omega |G(\beta,\gamma,y_1) - G(\beta,\gamma,y_2)|^2 \mathrm{dx} = \\
&= \int_\Omega \left| \left(\beta \int_\Omega |\nabla y_1|^2 \mathrm{dx} + \gamma\right)\Delta y_1 - \left(\beta\int_\Omega |\nabla y_2|^2 dx + \gamma\right)\Delta y_2 \right|^2 \mathrm{dx} \leq \\
&\leq 2\int_\Omega \Big| \Big(\beta \int_\Omega |\nabla y_1|^2 \mathrm{dx} + \gamma\Big)(\Delta y_1 - \Delta y_2) \Big|^2 \mathrm{dx} + \\
&+ 2\int_\Omega \Big| \Delta y_2 \Big(\beta\int_\Omega |\nabla y_1|^2 \mathrm{dx} + \gamma - \beta\int_\Omega |\nabla y_2|^2 \mathrm{dx} - \gamma\Big) \Big|^2 \mathrm{dx} \leq \\
&\leq 2\Big(\beta\int_\Omega |\nabla y_1|^2 \mathrm{dx} + \gamma\Big)^2 \int_\Omega |\Delta y_1 - \Delta y_2|^2 \mathrm{dx} + \\
&+ 2\Big(\int_\Omega |\Delta y_2|^2 dx\Big)\beta^2 \Big(\int_\Omega |\nabla(y_1 - y_2)||\nabla(y_1+y_2)|\mathrm{dx}\Big)^2 \leq \\
&\leq 2\Big(\beta\int_\Omega |\nabla y_1|^2 \mathrm{dx} + \gamma\Big)^2 \int_\Omega |\Delta y_1 - \Delta y_2|^2 \mathrm{dx} + \\
&+ 2\Big(\int_\Omega |\Delta y_2|^2 \mathrm{dx}\Big)\beta^2 \Big(\int_\Omega |\nabla(y_1 - y_2)|^2 \mathrm{dx}\Big)\Big(\int_\Omega |\nabla(y_1+y_2)|^2 \mathrm{dx}\Big) \leq \\
&\leq C(M_1,\gamma,\beta) d_\Omega^6 \int_\Omega |\Delta^2(y_1 - y_2)|^2 \mathrm{dx}.
\end{aligned} \tag{38}$$

Now, we compute I_2.

We can write the equation as follows:

$$
\begin{aligned}
I_2 &= 2\int_\Omega \lambda^2 ||f||^2_{\infty,\Omega}\left|\frac{1}{(1-y_1)^2 g(\chi,y_1)} - \frac{1}{(1-y_2)^2 g(\chi,y_2)}\right|^2 \mathrm{dx} \leq \\
&\leq 4\lambda^2 ||f||^2_{\infty,\Omega}\int_\Omega \left|\frac{1}{(1-y_1)^2 g(\chi,y_1)} - \frac{1}{(1-y_2)^2 g(\chi,y_1)}\right|^2 \mathrm{dx}+ \\
&+4\lambda^2 ||f||^2_{\infty,\Omega}\int_\Omega \left|\frac{1}{(1-y_2)^2 g(\chi,y_1)} - \frac{1}{(1-y_2)^2 g(\chi,y_2)}\right|^2 \mathrm{dx} \leq \\
&\leq \underbrace{4\lambda^2 ||f||^2_{\infty,\Omega}\int_\Omega \left|\frac{1}{(1-y_1)^2} - \frac{1}{(1-y_2)^2}\right|^2 \mathrm{dx}}_{I_{21}} + \\
&\underbrace{+4\lambda^2\chi^2 ||f||^2_{\infty,\Omega}\int_\Omega \frac{1}{(1-y_2)^4}\left|\frac{1}{\left(1+\chi\int_\Omega \frac{1}{(1-y_1)}\mathrm{dx}\right)^2} - \frac{1}{\left(1+\chi\int_\Omega \frac{1}{(1-y_2)}\mathrm{dx}\right)^2}\right|^2 \mathrm{dx}}_{I_{22}}.
\end{aligned} \tag{39}
$$

Let us now calculate I_{21}.

$$
\begin{aligned}
I_{21} &= 4\lambda^2 ||f||^2_{\infty,\Omega}\int_\Omega \left|\frac{1}{(1-y_1)^2} - \frac{1}{(1-y_2)^2}\right|^2 \mathrm{dx} = \\
&= 4\lambda^2 ||f||^2_{\infty,\Omega}\int_\Omega \frac{(y_1-y_2)^2((1-y_1)+(1-y_2))^2}{(1-y_1)^4(1-y_2)^4}\mathrm{dx} \leq \\
&\leq 16\lambda^2 ||f||^2_{\infty,\Omega} d^{*2}\int_\Omega \frac{(y_1-y_2)^2}{(1-y_1)^4(1-y_2)^4}\mathrm{dx} < \\
&< 16\lambda^2 ||f||^2_{\infty,\Omega} ||y_1-y_2||^2_{\infty,\Omega} d^{*2}\int_\Omega \frac{1}{(1-y_1)^4(1-y_2)^4}\mathrm{dx}.
\end{aligned} \tag{40}
$$

But being

$$
\begin{aligned}
&\int_\Omega \frac{1}{(1-y_1)^4(1-y_2)^4}\mathrm{dx} \leq \\
&\leq \left(\int_\Omega \frac{1}{(1-y_1)^8}\mathrm{dx}\right)^{\frac{1}{2}}\left(\int_\Omega \frac{1}{(1-y_2)^8}\mathrm{dx}\right)^{\frac{1}{2}} \leq \\
&\leq \left(\int_\Omega \frac{1}{(1-y_1)^{16}}\mathrm{dx}\right)^{\frac{1}{4}}(d^N_\Omega)^{\frac{1}{4}}\left(\int_\Omega \frac{1}{(1-y_2)^{16}}\mathrm{dx}\right)^{\frac{1}{4}}(d^N_\Omega)^{\frac{1}{4}},
\end{aligned} \tag{41}
$$

I_{21} becomes

$$
I_{21} = 16\lambda^2 d^{*2} ||f||^2_{\infty,\Omega} M^{\frac{1}{2}} (d^N_\Omega)^{\frac{1}{2}} ||y_1-y_2||^2_{\infty,\Omega}. \tag{42}
$$

Now, we calculate I_{22} (For this purpose, we exploit $a^2-b^2 < (2a-2b)^2$).

$$
\begin{aligned}
I_{22} = 4\lambda^2\chi^2||f||^2_{\infty,\Omega}\int_\Omega \frac{1}{(1-y_2)^4}\left|\frac{1}{\left(1+\chi\int_\Omega \frac{1}{(1-y_1)}\mathrm{dx}\right)^2} - \frac{1}{\left(1+\chi\int_\Omega \frac{1}{(1-y_2)}\mathrm{dx}\right)^2}\right|^2 \mathrm{dx} \leq \\
\leq 4\lambda^2\chi^2||f||^2_{\infty,\Omega}\int_\Omega \frac{1}{(1-y_2)^4}\left|\left(2\chi\int_\Omega \frac{1}{1-y_2}\mathrm{dx} - 2\chi\int_\Omega \frac{1}{1-y_1}\mathrm{dx}\right)^2\right|^2 \mathrm{dx} \leq \\
\leq 64\lambda^2\chi^6||f||^2_{\infty,\Omega}\int_\Omega \frac{1}{(1-y_2)^4}||y_2-y_1||^4_{\infty,\Omega}\left|\int_\Omega \frac{1}{(1-y_2)(1-y_1)}\mathrm{dx}\right|^4 \mathrm{dx} \leq \\
\leq 64\lambda^2\chi^6||f||^2_{\infty,\Omega}\int_\Omega \frac{1}{(1-y_2)^4}||y_2-y_1||^2_{\infty,\Omega}\left|\int_\Omega \frac{1}{(1-y_2)(1-y_1)}\mathrm{dx}\right|^4 \mathrm{dx} \leq \\
\leq 64\lambda^2\chi^6||f||^2_{\infty,\Omega}||y_2-y_1||^2_{\infty,\Omega}M^{\frac{1}{8}}d_\Omega^{\frac{13N}{16}}\int_\Omega \frac{1}{(1-y_2)^4}\mathrm{dx} \leq \\
\leq 64\lambda^2\chi^6||f||^2_{\infty,\Omega}||y_2-y_1||^2_{\infty,\Omega}M^{\frac{3}{8}}d_\Omega^{\frac{25N}{16}}
\end{aligned}
\tag{43}
$$

Therefore, taking into account both (42) and (43), (39) becomes the following equation:

$$
\begin{aligned}
I_2 \leq 16\lambda^2||f||^2_{\infty,\Omega}M^{\frac{1}{2}}(d_\Omega^N)^{\frac{1}{2}}||y_1-y_2||^2_{\infty,\Omega}d^{*2}+ \\
+64\lambda^2\chi^6||f||^2_{\infty,\Omega}||y_2-y_1||^2_{\infty,\Omega}M^{\frac{3}{8}}d_\Omega^{\frac{25N}{16}} = \\
= 16\lambda^2||f||^2_{\infty,\Omega}M^{\frac{3}{8}}(d_\Omega^N)^{\frac{1}{2}}\left(M^{\frac{1}{8}}d^{*2}+\chi^6\right)||y_1-y_2||^2_{\infty,\Omega}
\end{aligned}
\tag{44}
$$

According to the Sobolev immersion theorem (for details, see [23] p. 20 Theorem 3.1), and since $N \leq 3$, it follows that:

$$
\begin{aligned}
||y_1-y_2||^2_{\infty,\Omega} \leq C\Bigg(\frac{1}{(d_\Omega)^{\frac{N}{2}}}|y_1-y_2|_{0,\Omega}+ \\
+(d_\Omega)^{1-\frac{N}{2}}|y_1-y_2|_{1,\Omega}+(d_\Omega)^{2-\frac{N}{2}}|y_1-y_2|_{2,\Omega}\Bigg)^2
\end{aligned}
\tag{45}
$$

in which C is a constant, and d_Ω is the diameter of Ω. Moreover, by applying the Poincaré inequality to (45), we can easily achieve the following equation:

$$
||y_1-y_2||^2_{\infty,\Omega} \leq 3C(d_\Omega)^{4-N}|y_1-y_2|^2_{2,\Omega}. \tag{46}
$$

We observe that Ω is convex, so it is possible to apply the Miranda–Talenti inequality to (46), thus obtaining the following:

$$
||y_1-y_2||^2_{\infty,\Omega} \leq 9C(d_\Omega)^{4-N}|\Delta(y_1-y_2)|^2_{0,\Omega}. \tag{47}
$$

in which we have exploited both the Poincaré inequality and the fact that $|\Delta\cdot|_{0,\Omega}$ is a norm on $H^2 \cap H^1_0(\Omega)$ that, as is known, is equivalent to the standard Sobolev's norm [24]. We also observe that by exploiting the Marcinkiewicz interpolation theorem [25], one obtains the following for $u \in H^4 \cap H^1_0(\Omega)$:

$$
\int_\Omega |\nabla u|^2\mathrm{dx} \leq Cd^2_\Omega\int_\Omega |\Delta u|^2\mathrm{dx} \tag{48}
$$

$$
\int_\Omega |\Delta u|^2\mathrm{dx} \leq Cd^4_\Omega\int_\Omega |\Delta^2 u|^2\mathrm{dx}. \tag{49}
$$

It is worth nothing that $H^4 \subset C^0(\overline{\Omega})$, and moreover, $L^\infty \subset L^4$. Therefore, we can apply the same procedure as in the first case. Furthermore, $H^{4,4} \subset H^{2,2}$, thus $|y_1 - y_2|^2_{4,\Omega}$ can be increased, exploiting the Sobolev immersion theorem.

From (38), (48), and (49), we obtain:

$$\begin{aligned}
&\int_\Omega |G(\beta,\gamma,y_1) - G(\beta,\gamma,y_2)|^2 \mathrm{dx} \leq \\
&\leq 2\Big(\beta C d_\Omega^2 M_1 + \gamma\Big)^2 C d_\Omega^4 \left(\int_\Omega |\Delta^2(y_1 - y_2)|^2 \mathrm{dx} \right) + \\
&+ 8 C d_\Omega^6 M_1^2 \beta^2 \int_\Omega |\Delta^2(y_1 - y_2)|^2 \mathrm{dx}.
\end{aligned} \tag{50}$$

Moreover, from (44), we can write the following equation:

$$\begin{aligned}
I_2 &\leq 64\lambda^2 ||f||^2_{\infty,\Omega} M^{\frac{3}{8}} d_\Omega^{\frac{N}{2}} (d^{*2} M^{\frac{1}{8}} + \chi^6) ||y_1 - y_2||^2_{\infty,\Omega} = \\
&= C(\lambda,\chi,f,M) d_\Omega^{6N+4} \int_\Omega |\Delta(y_1 - y_2)|^2 \mathrm{dx} \leq \\
&\leq C(\lambda,\chi,M_1) d_\Omega^{6N+8} \int_\Omega |\Delta^2(y_1 - y_2)|^2 \mathrm{dx}.
\end{aligned} \tag{51}$$

Now, we compute I_3.

Considering Theorem 3.1 in [23] (p. 20), and as $N \leq 3$, it follows that $H^{3,2} \subset C^0(\overline{\Omega})$, from which we obtain the following:

$$\begin{aligned}
I_3 &= 2\lambda^2\delta^2 \int_\Omega \Big| |\nabla y_2|^2 - |\nabla y_2|^2 \Big|^2 \mathrm{dx} = \\
&= 2\lambda^2\delta^2 \int_\Omega \Big| (|\nabla y_1| - |\nabla y_2|)^2 (|\nabla y_1| + |\nabla y_2|)^2 \Big| \mathrm{dx} = \\
&= 2\lambda^2\delta^2 \int_\Omega |\nabla(y_1 - y_2)|^2 (|\nabla y_1| + |\nabla y_2|)^2 \mathrm{dx} \leq \\
&\leq 2\lambda^2\delta^2 \left(\int_\Omega |\nabla(y_1 - y_2)|^4 \mathrm{dx} \right)^{\frac{1}{2}} \left(\int_\Omega |\nabla(y_1 + y_2)|^4 \mathrm{dx} \right)^{\frac{1}{2}} \leq \\
&\leq 16\lambda^2\delta^2 \left(\int_\Omega |\nabla(y_1 - y_2)|^4 \mathrm{dx} \right)^{\frac{1}{2}} \left(\int_\Omega [|\nabla y_1|^4 + |\nabla y_2|^4] \mathrm{dx} \right)^{\frac{1}{2}} \leq \\
&\leq 16 C \lambda^2 \delta^2 M_2 \left(\int_\Omega |\nabla(y_1 - y_2)|^4 \mathrm{dx} \right)^{\frac{1}{2}}.
\end{aligned} \tag{52}$$

Applying Theorem 3.10 in [23] and the Marcinkiewicz interpolation theorem [26] from (52), we can write the equation as follows:

$$\begin{aligned} I_3 &\leq 16\delta^2\lambda^2 M_2\Big(||\nabla(y_1-y_2)||^4_{\infty,\Omega}\Big)^{\frac{1}{2}}(d_\Omega^{\frac{N}{2}})^{\frac{1}{2}} \leq \\ &\leq 16\delta^2\lambda^2 M_2 (d_\Omega)^{\frac{N}{2}}||\nabla(y_1-y_2)||^2_{\infty,\Omega} \leq \\ &\leq 16\delta^2\lambda^2 M_2 (d_\Omega)^{\frac{N}{2}}\Bigg(\frac{1}{(d_\Omega)^{\frac{N}{2}}}|\nabla(y_1-y_2)|_{0,\Omega} + (d_\Omega)^{1-\frac{N}{2}}|\nabla(y_1-y_2)|_{1,\Omega} + \\ &\quad + (d_\Omega)^{2-\frac{N}{2}}|\nabla(y_1-y_2)|_{2,\Omega}\Bigg)^2 \leq \\ &\leq 16\delta^2\lambda^2 M_2 d_\Omega^{2(2-\frac{N}{2})}(d_\Omega)^{\frac{N}{2}}|\nabla(y_1-y_2)|^2_{2,\Omega} \leq \\ &\leq 16\delta^2\lambda^2 M_2 d_\Omega^{2-\frac{N}{2}}|\Delta(y_1-y_2)|^2_{0,\Omega} = \\ &= 16\delta^2\lambda^2 M_2 d_\Omega^{6-\frac{N}{2}}|\Delta^2(y_1-y_2)|^2_{0,\Omega}. \end{aligned} \tag{53}$$

Finally, (37) becomes:

$$\begin{aligned} &\int_\Omega \Big|B(y_1) - B(y_2) - (F((\beta,\gamma,\chi,f,y_1) - F(\beta,\gamma,\chi,f,y_2))\Big|^2 \mathrm{dx} \leq \\ &\leq C(\beta,\lambda,\gamma,\delta,\chi,M,M_1,M_2,f) d_\Omega^{\frac{N}{2}} \int_\Omega \Big|B(y_1) - B(y_2)\Big|^2 \mathrm{dx}. \end{aligned} \tag{54}$$

Therefore, Assumption (iii) is also verified. In fact, as $d_\Omega \ll 1$, we set the following:

$$K_2 = C(\beta,\lambda,\gamma,\delta,\chi,M,M_1,M_2,f) d_\Omega^{\frac{N}{2}} < 1. \tag{55}$$

Then, the proof is to be considered concluded.

Remark 9. *We observe that $K_2 < 1$ makes sense because $d_\Omega \ll 1$. Thus, $d_\Omega^{\frac{N}{2}} \ll 1$. Therefore, from (55), it follows that:*

$$k_2 = C(\beta,\lambda,\gamma,\delta,\chi,M,M_1,M_2,f) < d_\Omega^{-\frac{N}{2}}. \tag{56}$$

As $d_\Omega \ll 1$, then $d_\Omega^{-\frac{N}{2}} \gg 1$. This means that:

$$K_2 \in [0, d_\Omega^{-\frac{N}{2}}) \tag{57}$$

where $[0, d_\Omega^{-\frac{N}{2}})$ represents a rather wide range of values. In other words, it is reasonable to think that there are many devices whose deformable plate constituent electromechanical parameters (β, γ, χ, f), together with the operating circuit conditions (λ and δ), match the condition (56).

7. Possible Intended Uses of the MEMS Device Under Study

The device studied here does not require particular precautions for its construction and therefore its industrial production, in our opinion, would be characterized by rather low costs. Furthermore, as mentioned in Section 3, the MEMS device studied in this paper can be used in all those industrial applications where the operating voltage V is reduced. Then, the most suitable uses for this device are, for example, biomedical applications where the required V values are usually limited. Among them the micropumps stand out, which are used for the intravenous administration of drugs, which, as is known, require microdevices equipped with mobile elements. Moreover, the device studied here could be used in precision surgical microsystems: by correctly applying sequential actuation

to the electrostatic clamps, the deformable plate would help create the movement. Obviously, the actual quantification of V will be decisive in order to select the most correct intended use. It is worth noting that the variety of parallel plate MEMS devices is wide and ever increasing. In addition, an ever-increasing number of MEMS devices is being incorporated into functional systems. Diversity, cost, and compatibility with integrated circuit manufacturing technologies determine their dominant presence on the market. We also observed that MEMS devices include both electronic and mechanical parts. However, most of the acceptance tests are electronic, so one of the greatest difficulties associated with this technology is represented by mechanical testing. We observe that electrostatic MEMS sensors use small mechanical and electrical components integrated into a single chip by combining microelectronics with the mechanics of micro sensors. In recent years, this technology has seen strong growth, with numerous companies producing devices and development tools used in the most varied of fields such as information, robotics, and electronics. A field of application, for example, could be in metropolitan areas, particularly in the Smart Cities field, which has already begun to decline in multiple IoT applications.

8. Conclusions

In the present work, a new nonlocal physico-mathematical model for electrostatic MEMS devices with parallel metal plates has been proposed and studied, and in which an additive term for the fringing field has been obtained by the Pelesko–Driscoll approach. The model obtained, controlled in external voltage by means of a capacitive control circuit, takes into account the effects resulting from the fringing field by means of an addend that can be easily implemented both via software and hardware, making the model complete and attractive for any industrial application. In addition, given the presence of some specific parameters, the model takes into account both the effects due to any problems of stiffness and self-stretching of the deformable element, and any sudden excesses in tension, proposing the device under study for possible use in the biomecal and robotics fields where the intended application requires a voltage that is limited in amplitude. The model obtained, even if complete, does not allow for the explicit acquisition of its solutions (profiles of the deformable plate) for which we have worked, analytically demonstrating that it admits a single solution. Thus, we obtained analytical conditions that, if verified by any approximate numerical solutions, the latter would not represent ghost solutions. Furthermore, the fact of having proved that the model admits a unique solution demonstrates that for each value of external V (with limited amplitude), there is one and only one position for the deformed plate, making this model attractive for any industrial applications (in biomedical and robotic equipment). Particularly, it has been proved that the model admits unique nonlocal solutions using a well-known result proved in the framework of topological spaces. The results obtained, being valid for $N < 4$, are also valid for thin dielectric layers where they are generally representable in one-dimensional geometries ($N = 1$) in which the fringing field effects are very relevant.

9. Some Future Perspectives

We observe that the proposed model, relative to δ that weighs the effects due to the fringing field phenomenon, is not explicitly controllable in voltage, so it would be advisable to study the control problem in the future as well to avoid the possible triggering of discharges in the dielectric. Furthermore, with regard to industrial production, before implementing a device in hardware, its software design is required through the use of suitable numerical techniques. So, in the near future, it would be advisable to study the proposed model with numerical techniques in order to obtain approximate solutions that satisfy the conditions of existence and uniqueness obtained in this paper (avoiding any ghost solutions). Moreover, there is no doubt that the proposed model requires a dynamic upgrade in order to obtain the conditions of existence and uniqueness of the deforming plate profile that are also dependent on time, making the device attractive for all those industrial applications in which timing represents a decisive action. Finally, it

is worth noting that the model presented here, although very close to the physical reality of electrostatic MEMS with parallel plates, is extremely complex. As such, it does not allow for routine analytical studies to be performed on it. Then, there would be a need to implement some simplifications in the geometry of the device so that the model that would be obtained (simpler than the starting model) could be studied mathematically. But in this case, the results obtained are unlikely to agree with any experimental data. Hence, experience suggests that we could only take advantage of any qualitative indications of the behavior of the MEMS device characterized by the simplifications mentioned above.

Author Contributions: Conceptualization, P.D.B., L.F., and M.V.; methodology, L.F. and M.V.; validation, P.D.B. and L.F.; formal analysis, L.F. and M.V.; investigation, P.D.B. and M.V.; resources, P.D.B., L.F., and M.V.; writing—original draft preparation, M.V.; writing—review and editing, P.D.B. and L.F.; supervision, P.D.B., L.F., and M.V. All authors have read and agreed to the published version of the manuscript.

Funding: This research received no external funding.

Institutional Review Board Statement: Not applicable.

Informed Consent Statement: Not applicable.

Conflicts of Interest: The authors declare no conflicts of interest. Luisa Fattorusso is a member of the National Group for Mathematical Analysis, Probability, and their Applications (GNAMPA-INdAM).

Abbreviations

The following abbreviations are used in this manuscript:

MEMS	micro-electro-mechanical systems
V	electrostatic potential
λ	drop-in voltage
δ	the real parameter that weighs the effect of the fringing field
Ω	smooth bounded domain
u	unknown profile of the deflecting plate
f	bounded functions related to the dielectric properties of the plates
$\tilde{K}_1(x)$, $\tilde{K}_2(x)$	specific weight functions
d	distance between the plates in the MEMS
L	the length of the MEMS
T	the mechanical tension of the deformable plate at rest
ϵ_0	the permittivity of free space
$\tilde{F}(x)$	load function
V_s	source voltage
C_f	the capacitance of the fixed series capacitor
C	the capacitance of the MEMS device
χ	the dimensionless parameter that weighs the capacitance of the MEMS
$E_s(u(x))$	stretching energy
γ	stretching parameter
D	flexural rigidity

References

1. Pelesko, J.A. *Modeling MEMS and NEMS*; Chapman & Hall/CRC: Boca Raton, FL, USA; London, UK; New York, NY, USA; Washington, DC, USA, 1998.
2. Korvink, J. Paul, O. *MEMS: A Practical Guide to Design, Analysis, and Applications*; Springer: Berlin/Heidelberg, Germany, 2006.
3. Li, Y.; Li, H.; Xiao, Y.; Cao, L.; Guo, Z.S. A Compensation Method for Nonlinear Vibration of Silicon-Micro Resonant Sensor. *Sensors* **2021** *21*, 2545. [CrossRef]
4. Versaci, M.; Morabito, F.C. Fuzzy time series approach for disruption prediction in Tokamak reactors. *IEEE Trans. Magn.* **2003** *39*, 1503–1506. [CrossRef]
5. Fan, X.; Smith, A.D.; Forsberg, F.; Wagner, S.; Schröder, S.; Akbari, S.S.A.; Fischer, A.C.; Villanueva, L.G.; Östling, M.; Lemme, M.C.; et al. Manufacture and Characterization of Graphene Membrane with Suspended Silicon Proof Masses for MEMS and NEMS Applications. *Microsyst. Nanoeng.* **2020** *6*, 17. [CrossRef]

6. Versaci, M.; Jannelli, A.; Morabito, F.C.; Angiulli, G. A Semi-Linear Elliptic Model for a Circular Membrane MEMS Device Considering the Effect of the Fringing Field. *Sensors* **2021**, *21*, 5237. [CrossRef] [PubMed]
7. Li, Z.; Gao, S.; Jin, L.; Liu, H.; Niu, S. Micromachined Vibrating Ring Gyroscope Architecture with High-Linearity, Low Quadrature Error and Improved Mode Ordering. *Sensors* **2021**, *20*, 4327. [CrossRef] [PubMed]
8. Podbiel, D.; Laermer, F.; Zengerle, R.; Hoffmann, J. Fusing MEMS Technology with Lab-on-Chip: Nanoliter-Scale Silicon Microcavity Arrays for Digital DNA Quantification and Multiplex Testing. *Microsyst. Nanoeng.* **2020**, *6*, 328–341. [CrossRef] [PubMed]
9. Zhou, N.; Jia, P.; Liu, J.; Ren, Q.G.A.; Liang, T.; Xiong, J. MEMS-Based Reflective Intensity-Modulated Fiber-Optic Sensor for Pressure Measurements. *Sensors* **2020**, *20*, 2233. [CrossRef] [PubMed]
10. Alodhayb, A. Modeling of an Optically Heated MEMS-Based Micromechanical Bimaterial Sensor for Heat Capacitance Measurements of Single Biological Cells. *Sensors* **2020**, *20*, 215. [CrossRef] [PubMed]
11. Maruyama, S.; Hizawa, T.; Takahashi, K.; Sawada, K. Optical-Interferometry-Based CMOS-MEMS Sensor Transduced by Stress-Induced Nanomechanical Deflection. *Sensors* **2018**, *18*, 138. [CrossRef] [PubMed]
12. Din, H.; Iqbal, F.; Lee, B. Design Approach for Reducing Cross-Axis Sensitivity in a Single-Drive Multi-Axis MEMS Gyroscope. *Micromachines* **2021**, *12*, 902. [CrossRef] [PubMed]
13. Fitzgerald, A.; Chung, C.C. *MEMS Product Development*; Springer: Zurich, Switzerland, 2021.
14. Cassani, D.; Fattorusso, L.; Tarsia, A. Global Existence for Nonlocal MEMS. *Nonlinear Anal.* **2011**, *74*, 5722–5726. [CrossRef]
15. Hashimoto, K.; Shiotani, T.; Mitsuya, H.; Chang, K.C. MEMS Vibrational Power Generator for Bridge Slab and Pier Health Monitoring *Appl. Sci.* **2020**, *10*, 8258.
16. Petre, A.R.; Craciunescu, R.; Fratu, O. Design, Implementation and Simulation of a Fringing Field Capacitive Humidity Sensor *Sensors* **2020**, *20* , 5644. [CrossRef] [PubMed]
17. Pelesko, J.A.; Driscoll, T.A. The Effect of the Small-Aspect-Ratio Approximation on Canonical Electrostatic MEMS Models. *J. Eng. Math.* **2005**, *53*, 239–252. [CrossRef]
18. Wei, J.; Ye, D. On MEMS Equation with Fringing Field. *Proc. Am. Math. Soc.* **2010**, *138*, 1693–1699. [CrossRef]
19. Pelesko, J.A.; Triolo, A.A. Nonlocal Problems in MEMS Device Control. *J. Eng. Math.* **2001**, *41*, 345–366. [CrossRef]
20. Cassani, D.; d'O, J.M.; Ghoussoub, N. On a Fourth Order Elliptic Problem with a Singular Nonlinearity. *Adv. Nonlinear Stud.* **2011**, *9*, 189–209. [CrossRef]
21. Berchio, E.; Cassani, D.; Gazzola, F. Hardy-Rellich Inequalities with Boundary Remainder Terms and Applications. *Manuscripta Math.* **2010**, *131*, 427–458. [CrossRef]
22. Tarsia, A. Differential Equations and Implicit Functions: a Generalization of the Near Operator Theorem. *Topol. Methods Nonlinear Anal.* **1998**, *11*, 115–133. [CrossRef]
23. Campanato, S. *Sistemi Ellittici in Forma Divergenza: Regolaritá all'Interno*; Scuola Normale Superiore di Pisa: Pisa, Italy, 1980.
24. Cassani, D.; Kaltenbacher, B.; Lorenzi A. Direct and Inverse Problems Related to MEMS. *Inverse Probl.* **2009**, *25*, 1–22. [CrossRef]
25. Brezis, H. *Functional Analysis, Sobolev Spaces and Partial Differential Equations*; Springer: New York, NY, USA, 2011.
26. Burenkov, V. *Sobolev Spaces on Domains*; Vieweg+Teubner Verlag, Wiesbaden, Germany, 1998.